Adaptive LES of 3D decaying isotropic turbulence

By Daniel E. Goldstein†, Oleg V. Vasilyev†, Nicholas K.-R. Kevlahan‡

In this work SCALES simulations of decaying incompressible isotropic turbulence are compared to DNS and LES results. Current Large Eddy Simulation (LES) relies on, at best, a zonally adapted filter width to reduce the computational cost of simulating complex turbulent flows. While an improvement over a uniform filter width, this approach has two limitations. First, it does not capture the high wave number components of the coherent vortices that make up the organized part of turbulent flows, thus losing essential physical information. Secondly, the flow is over-resolved in the regions between the coherent vortices, thus wasting computational resources. The Stochastic Coherent Adaptive Large Eddy Simulation (SCALES) approach addresses these shortcomings of LES by using a dynamic grid adaptation strategy that is able to resolve and "track" the most energetic coherent structures in a turbulent flow field. This corresponds to a dynamically adaptive local filter width. Unlike Coherent Vortex Simulation (CVS), which is able to recover low order statistics with no subgrid scale stress model, the higher compression used in SCALES necessitates that the effect of the unresolved subgrid scale (SGS) stresses must be modeled. These SGS stresses are approximated using a new dynamic eddy viscosity model based on Germano's classical dynamic procedure redefined in terms of two wavelet thresholding filters.

1. Introduction

Turbulence is characterized by energetic eddies that are localized in space and scale, yet most numerical methods for turbulent flow simulations do not take advantage of this localization. In this work we explore the possibility of making use of this localization by "compressing" the turbulence problem such that a simulation with a subset of the total modes captures the dynamics of the most energetic eddies in the flow. A recent method for simulating turbulence called Coherent Vortex Simulation (CVS), introduced by Farge *et al.* (Farge *et al.* 1999), uses a wavelet filter to dynamically resolve and "track" the energetic coherent eddies or vortices in a turbulent flow. It has been shown that the resulting subgrid scale (SGS) field with CVS is near Gaussian white noise (Goldstein & Vasilyev 2004, Farge *et al.* 2001), which results in practically no SGS dissipation. Therefore, a CVS simulation can be run with no SGS model if only low order statistics are required. It is important to note that there is still significant energy transfer between the resolved and SGS modes and visa-versa, but the statistical average or net energy transfer is zero. If higher order statistics are required, then a purely stochastic subgrid scale stress model can be used to reproduce the effect of the subgrid scales. One of the challenges with the CVS method is how to determine on the fly during an actual simulation the "ideal" wavelet compression, which results in a purely incoherent subgrid scale field. Even if it can be found in a cost effective manner it is still likely that the

† University of Colorado at Boulder, CO
‡ McMaster University at Hamilton, ON, Canada

associated adaptive grid will be too fine to be cost effective for simulating high Re number flows since the computational cost of CVS falls between DNS and LES.

Recently a new methodology called Stochastic Coherent Adaptive Large Eddy Simulation (SCALES) (Goldstein & Vasilyev 2004) has been introduced that shares the CVS methods ability to dynamically resolve and "track" the most energetic part of the coherent eddies in a turbulent flow field with the higher computational efficiency associated with LES. With SCALES the maximum number of modes in the simulation are resolved, given the balance between computing resources and user defined acceptable simulation error. Thus, with SCALES the collocation grid dynamically adapts to the local flow in order to resolve the maximum portion of the coherent energetic eddies possible given the *a priori* wavelet filter threshold (ϵ) specified. With a field compression in the range of that used with typical LES applications the SGS modes are no longer near Gaussian white noise, as with CVS, so a SGS model is required. Yet at the same field compression as LES, using a spectral cutoff filter, the wavelet filter used with SCALES results in a significantly reduced level of total SGS dissipation that will have to be modeled (Goldstein & Vasilyev 2004). In this work we apply the Stochastic Coherent Adaptive Large Eddy Simulation (SCALES) method to the problem of three-dimensional decaying isotropic turbulence.

An eddy viscosity type SGS model for SCALES is also investigated in this work. Since the wavelet threshold filter lacks a clearly defined global filter width, an alternative model scaling based on the wavelet theshold parameter (ϵ) is proposed. Results using a modified Smagorinsky (Smagorinsky 1963) eddy viscosity SGS stress model using both a constant model coefficient and a dynamic coefficient determined by a new dynamic procedure are shown. This new dynamic procedure follows the derivation of Germano's (Germano *et al.* 1991, Germano 1992) classical dynamic procedure. Test filtering is defined as a wavelet filter with threshold equal to 2ϵ and an explicit grid filter is used with a wavelet filter threshold value of ϵ.

In this research the SCALES method has been implemented using a Dynamically Adaptive Wavelet Collocation (DAWC) method (Vasilyev 2003, Vasilyev & Bowman 2000). A DAWC method is ideal for implementing the SCALES methodology as it combines the resolution of the energetic coherent modes in a turbulent flow with the simulation of their temporal evolution (Vasilyev 2003, Vasilyev & Bowman 2000, Kevlahan *et al.* 2003, Goldstein *et al.* 2003, Vasilyev & Kevlahan 2002). The wavelet collocation method employs wavelet compression as an integral part of the solution such that the solution is obtained with the minimum number of grid points for a given accuracy.

The rest of this paper is organized as follows. In section 2 background theory and results relevant to this work are presented. In Section 3 a Dynamically Adaptive Wavelet Collocation Solver is introduced that has been used to implement the SCALES method. In Section 4 the implementation of SCALES along with the introduction of a new dynamic SGS model is presented. Then in Section 5 fully adaptive SCALES simulations of three-dimensional decaying incompressible isotropic turbulence based on the DAWC method are presented. In the final section conclusions and discussion of future work are provided.

2. Background

2.1. *General Properties of Wavelets*

Wavelets are basis functions, which are localized in both physical space (due to their finite support) and wavenumber space. For comparison, the classical Fourier transform is based

on functions (sines and cosines) that are well localized in frequency but do not provide localization in physical space due to their global support. Because of this space/scale localization, the wavelet transform provides both spatial and scale (frequency) information while the Fourier transform on the other hand only provides frequency information.

A field $u(\mathbf{x})$ can be represented in terms of wavelet basis functions as

$$u(\mathbf{x}) = \sum_{\mathbf{l}\in\mathcal{L}^0} c^0_{\mathbf{l}}\phi^0_{\mathbf{l}}(\mathbf{x}) + \sum_{j=0}^{+\infty}\sum_{\mu=1}^{2^n-1}\sum_{\mathbf{k}\in\mathcal{K}^{\mu,j}} d^{\mu,j}_{\mathbf{k}}\psi^{\mu,j}_{\mathbf{k}}(\mathbf{x})\,, \tag{2.1}$$

where $\phi^0_{\mathbf{k}}(\mathbf{x})$ and $\psi^{\mu,j}_{\mathbf{l}}$ are respectively n-dimensional scaling functions and wavelets of different families (μ) and levels of resolution (j). One may think of a wavelet decomposition as a multilevel or multiresolution representation of a function, where each level of resolution j (except the coarsest one) consists of wavelets $\psi^j_{\mathbf{l}}$ or family of wavelets $\psi^{\mu,j}_{\mathbf{l}}$ having the same scale but located at different positions. Scaling function coefficients represent the averaged values of the field, while the wavelet coefficients represent the details of the field at different scales. The wavelet functions have a zero mean, while the scaling functions do not. Note that in n-dimensions there are 2^n-1 distinctive n-dimensional wavelets (Daubechies 1992). Also note that due to the local support of both scaling functions and wavelets, there is a one-to-one correspondence between the location of each scaling function or wavelet with a grid point. As a result each scaling function coefficient $c^0_{\mathbf{l}}$ and each wavelet coefficient $d^{\mu,j}_{\mathbf{k}}$ is uniquely associated with a single grid point with the indices $\mathbf{l}$ and $\mathbf{k}$ respectively.

For this study we use a set of second generation wavelets known in the literature as lifted interpolating wavelets (Vasilyev & Bowman 2000, Sweldens 1996). In particular, simulations with the Dynamically Adaptive Wavelet Collocation (DAWC) solver are run using a lifted interpolating wavelet of order 6. For a more in-depth discussion on the construction of these wavelets the reader is referred to the papers by Sweldens (Sweldens 1996, Sweldens 1998) and Vasilyev and Bowman (Vasilyev & Bowman 2000). For a more general discussion on wavelets we refer to the books of Daubechies (1992) and Mallat (1999).

2.2. *Wavelet Filters*

Wavelet filtering is performed in wavelet space using wavelet coefficient thresholding, which can be considered as a non-linear filter that depends on each flow realization. The wavelet thresholding filter is defined by,

$$u_{\geqslant}(\mathbf{x}) = \sum_{\mathbf{l}\in\mathcal{L}^0} c^0_{\mathbf{l}}\phi^0_{\mathbf{l}}(\mathbf{x}) + \sum_{j=0}^{+\infty}\sum_{\mu=1}^{2^n-1}\sum_{\substack{\mathbf{k}\in\mathcal{K}^{\mu,j}\\ |d^{\mu,j}_{\mathbf{k}}|\geqslant\epsilon}} d^{\mu,j}_{\mathbf{k}}\psi^{\mu,j}_{\mathbf{k}}(\mathbf{x})\,. \tag{2.2}$$

The reconstruction error due to wavelet filtering with threshold ϵ can be shown to be (Vasilyev 2002, Donoho 1992):

$$||u(\mathbf{x}) - u_{\geqslant}(\mathbf{x})|| \leqslant C\epsilon\,, \tag{2.3}$$

for a sufficiently smooth function $u(\mathbf{x})$, where C is of order unity.

An important property of the wavelet thresholding filter is that in a dynamic simulation the grid required to support the wavelet filtered field will be changing in time and it will be collocated with the resolved wavelet coefficients. Thus, the grid defined by the wavelet

collocation points will track the areas of locally significant energy in physical space. Yet it is important to note that, unlike the Fourier modes, there is no one-to-one correspondence between wave number and wavelet level. Instead each wavelet level represents a region of wave numbers (Goldstein & Vasilyev 2004).

2.3. *Wavelet Compression and Wavelet De-noising*

The major strength of wavelet filtering decomposition (Eq. 2.2), is the ability to compress signals. For functions that contain isolated small scales on a large-scale background, most wavelet coefficients are small, thus, we can retain good approximation even after discarding a large number of wavelets with small coefficients. Intuitively, the coefficient $d_{\mathbf{l}}^{\mu,j}$ will be small unless $u(\mathbf{x})$ has variation on the scale of j in the immediate vicinity of wavelet $\psi_{\mathbf{l}}^{\mu,j}(\mathbf{x})$.

Another important property of wavelet analysis used in this work is the ability of wavelets to de-noise signals. The wavelet de-noising procedure, also called wavelet-shrinkage, originally introduced by Donoho (1993, 1994), can be briefly described as following: given a function that consists of a smooth function with superimposed noise, one performs a forward wavelet transform and sets to zero "noisy" wavelet coefficients, if the square of the wavelet coefficient is less than the noise variance σ^2, otherwise the wavelet coefficient is kept. This procedure is known as hard or linear thresholding. Donoho (1993) demonstrated that hard thresholding is optimal for de-noising signals in the presence of Gaussian white noise, because wavelet-based estimators minimize the maximal L^2-error for functions with inhomogeneous regularity. In the CVS method discussed in this work the "noise" is actually the SGS modes.

3. Dynamically Adaptive Wavelet Collocation Method

A key component in the implementation of the SCALES method has been a Dynamically Adaptive Wavelet Collocation (DAWC) (Vasilyev 2003, Vasilyev & Bowman 2000, Vasilyev & Kevlahan 2002, Vasilyev & Paolucci 1997) solver that is ideally suited to the simulation of turbulence since wavelets adapt the numerical resolution naturally to the localized turbulent structures that exist at all wave numbers in fully developed turbulence. The wavelet collocation method takes advantage of the fact that wavelets are localized in both space and scale, and as a result, functions with localized regions of sharp transition are well compressed using wavelet decomposition. The adaptation is achieved by retaining only those wavelets, whose coefficients are greater than an *a priori* given threshold (ϵ). Thus, high resolution computations are carried out only in those regions, where sharp transitions occur. With this adaptation strategy, a solution is obtained on a near optimal grid that "tracks" the coherent vortices in the field, *i.e.* far fewer grid points are needed for wavelets than for conventional finite-difference, finite-element, or spectral methods. By varying the threshold parameter ϵ this method can be used to implement any of the wavelet based methods discussed above, namely CVS or SCALES. The dynamically adaptive wavelet collocation algorithm has already been successfully applied to the solution of thermoacoustic wave propagation problems (Vasilyev & Paolucci 1997, Vasilyev & Paolucci 1996), combustion problems (Vasilyev & Bowman 2000, Vasilyev 2003, fluid-structure interaction problems (Vasilyev & Kevlahan 2002), viscoelastic flows (Vasilyev *et al.* 1997, Vasilyev *et al.* 2001), and the compaction phenomenon in poro-viscoelastic matrix (Vasilyev *et al.* 1998).

Let us briefly outline the main features of the numerical method. Details can be found

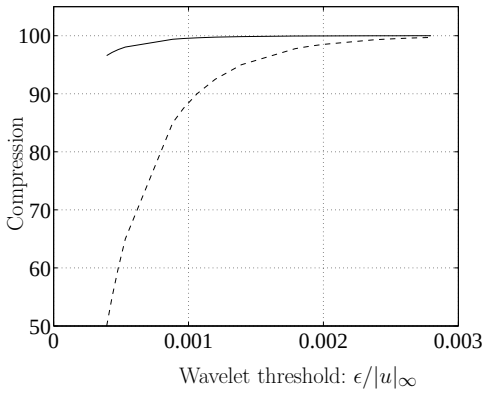

FIGURE 1. Field compression vs. normalized wavelet threshold $\epsilon/|u|_\infty$ using velocity wavelet filtering without adjacent zone (———) and with adjacent zone (- - - -) for field F_{256}. It can be seen that as ϵ increases the loss in compression due to the adjacent zone becomes less significant.

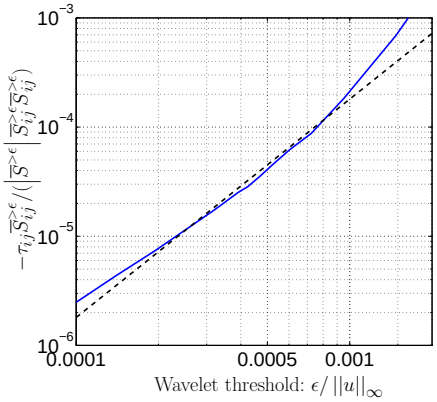

FIGURE 2. $\tau_{ij}\overline{S}_{ij}^{>\epsilon}/(\ \overline{S}^{>\epsilon}\ \overline{S}_{ij}^{>\epsilon}\overline{S}_{ij}^{>\epsilon})$ vs. normalized wavelet threshold $\epsilon/\left|\left|u\right|\right|_\infty$ using velocity wavelet filtering without adjacent zone (———) for field F_{256}. The dashed line is $(\epsilon/\left|\left|u\right|\right|_\infty)^2$. This range of $\epsilon/\left|\left|u\right|\right|_\infty$ corresponds to a field compression over the range of 78.5% to 99.95%. It can be seen that $\tau_{ij}\overline{S}_{ij}^{>\epsilon}/(\ \overline{S}^{>\epsilon}\ \overline{S}_{ij}^{>\epsilon}\overline{S}_{ij}^{>\epsilon})$ scales roughly as ϵ^2. The scaling begins to deviate at $\epsilon/\left|\left|u\right|\right|_\infty = 0.001$, which corresponds to 99.4% compression.

in Refs. Vasilyev 2003 or Vasilyev & Bowman 2000. In the wavelet collocation method there is a one-to-one correspondence between grid points and wavelets, which makes calculation of nonlinear terms simple and allows the grid to adapt automatically and dynamically to the solution by adding or removing wavelets. Very briefly, at each time step we take the wavelet transform of the solution, remove all wavelets with coefficient magnitude less than a threshold ϵ, and then reconstruct the solution. It can be shown that the L_∞ error of this approximation is $O(\epsilon)$. To account for the evolution of the solution over one time step the computational grid needs to be extended to include grid points associated with wavelets whose coefficients are or can possibly become significant during the next iteration (Vasilyev & Kevlahan 2003). To do this we add grid points that are adjacent in both position and scale to each significant wavelet coefficient. While the cost of this added adjacent zone is significant at low compression ratios it becomes much less so at higher compression ratios. This diminishing cost of the adjacent zone with increased compression will be the case for any numerical problem that has inherent local structures that dominate the field being simulated. Figure 1 shows the compression ratio vs. the wavelet filter threshold ϵ for a wavelet collocation grid adapted to a DNS field of isotropic turbulence ($\mathrm{Re}_\lambda = 72$) with and without an adjacent zone. We can see clearly that the added overhead of the adjacent zone becomes insignificant for compression ratios over 98%. This is the case because in turbulent flows, like the one considered, the the flow is dominated by localized energetic coherent vortices. Since each wavelet corresponds to a single grid point this procedure allows the grid to automatically follow the evolution of the solution in position and scale. We use second generation wavelets (Sweldens 1998), which allow the order of the wavelet (and hence of the numerical method) to be easily

varied. The method has a computational complexity $O(N)$, where N is the number of wavelets retained in the calculation (*i.e.* those wavelets with coefficients greater than ϵ plus nearest neighbors).

In summary, the dynamically adaptive wavelet collocation method is an adaptive, variable order method for solving partial differential equations with localized structures that change their location and scale in space and time. Because the computational grid automatically adapts to the solution (in position and scale), we do not have to know *a priori* where the regions of high gradients or structures exist. In related work the dynamically adaptive wavelet collocation method has been combined with the Brinkman penalization method (Kevlahan & Ghidaglia 2001, Vasilyev & Kevlahan 2003) to define solid structures in the domain for the simulation of complex geometry flows.

4. SCALES Implementation

The SCALES method is based on the premise that the most energetic coherent vortices (or structures) of a turbulent flow dominate mixing, heat transfer and other quantities of engineering interest, while the smaller incoherent background is only of interest because of how they effect the energetic coherent vortices (Goldstein & Vasilyev 2004). The SCALES equations for incompressible flow, that describe the evolution of the most energetic coherent vortices in the flow field, can be written as:

$$\frac{\partial \overline{u_i}^{>\epsilon}}{\partial x_i} = 0\,, \tag{4.1}$$

$$\frac{\partial \overline{u_i}^{>\epsilon}}{\partial t} + \frac{\partial (\overline{u_i}^{>\epsilon}\,\overline{u_j}^{>\epsilon})}{\partial x_j} = -\frac{1}{\rho}\frac{\partial \overline{p}^{>\epsilon}}{\partial x_i} + \nu \frac{\partial^2 \overline{u_i}^{>\epsilon}}{\partial x_j \partial x_j} - \frac{\partial \overline{\tau_{ij}}^{>\epsilon}}{\partial x_j}\,, \tag{4.2}$$

where

$$\overline{\tau_{ij}}^{>\epsilon} = \overline{u_i u_j}^{>\epsilon} - \overline{u_i}^{>\epsilon}\,\overline{u_j}^{>\epsilon} \tag{4.3}$$

and u_i is the velocity field, ρ is density, ν is kinematic viscosity, p is pressure and $\overline{(\cdot)}^{>\epsilon}$ represents spatial filtering with a wavelet thresholding filter. As a result of the filtering process the unresolved quantity $\overline{\tau_{ij}}^{>\epsilon}$, commonly referred to as the Subgrid Scale (SGS) stress, is introduced. Note that $\overline{\tau_{ij}}^{>\epsilon}$ is a function of the unfiltered velocity field u_i. However in order to close Eqs. 4.1-4.2 and realize the benefit of SCALES, a low order model for the SGS stress, which is based on the resolved quantities, is needed.

4.1. *SCALES SGS Modeling*

The standard Smagorinsky (Smagorinsky 1963) eddy viscosity SGS stress model defines an eddy viscosity that is proportional to the filter width and the characteristic filtered rate of strain. In the case of the non-linear wavelet thresholding filter used in SCALES there is no clearly defined filter width, so instead the wavelet threshold (ϵ) is used to properly scale the eddy viscosity:

$$\nu_T = C_s \epsilon^{\alpha} \left| \overline{S}^{>\epsilon} \right|, \tag{4.4}$$

where

$$\overline{S_{ij}}^{>\epsilon} = \frac{1}{2}\left(\frac{\partial \overline{u_i}^{>\epsilon}}{\partial x_j} + \frac{\partial \overline{u_j}^{>\epsilon}}{\partial x_i} \right), \tag{4.5}$$

is the strain rate of the resolved scales. We will show in Section 4.2 that appropriate scaling is obtained with $\alpha = 2$. The new linear eddy viscosity model is then used to

define a model for the subgrid scale stress (Eq. 4.3),

$$\overline{\tau_{ij}^M}^{>\epsilon} \equiv -2\nu_T \overline{S_{ij}}^{>\epsilon} , \tag{4.6}$$

where ν_T is the turbulent eddy viscosity.

The new Germano dynamic formulation for the model coefficient C_s is based on the wavelet filter threshold parameter (ϵ). For the dynamic procedure the grid filter is defined as $\overline{(\cdot)}^{>\epsilon}$ and the "test" filter is defined as $\overline{(\cdot)}^{>2\epsilon}$. The adjacent zone is excluded in both cases to obtain the proper model scaling. The dynamic procedure is then based on the original SGS stress, Eq. 4.3, and an alternative subgrid scale stress,

$$\overline{T_{ij}}^{>2\epsilon} = \overline{\overline{u_i u_j}^{>\epsilon}}^{>2\epsilon} - \overline{\overline{u_i}^{>\epsilon}}^{>2\epsilon} \overline{\overline{u_j}^{>\epsilon}}^{>2\epsilon} , \tag{4.7}$$

which would result from applying the wavelet thresholding"test" filter ($\overline{(\cdot)}^{>2\epsilon}$) to Eqs. 4.1-4.3. Note that the wavelet filter is a projection operator so by definition:

$$\overline{(\cdot)}^{>\epsilon_C} \equiv \overline{\overline{(\cdot)}^{>\epsilon_A}}^{>\epsilon_B} , \tag{4.8}$$

where

$$\epsilon_C = \max(\epsilon_A, \epsilon_B) . \tag{4.9}$$

Filtering Eq.4.3 at the "test" filter level and subtracting it from Eq.4.7 results in the modified Germano's identity (Germano 1992)

$$\overline{T_{ij}}^{>2\epsilon} - \overline{\overline{\tau_{ij}}^{>\epsilon}}^{>2\epsilon} = \overline{\overline{u_i}^{>\epsilon} \overline{u_j}^{>\epsilon}}^{>2\epsilon} - \overline{\overline{u_i}^{>\epsilon}}^{>2\epsilon} \overline{\overline{u_j}^{>\epsilon}}^{>2\epsilon} . \tag{4.10}$$

Then we can equate the modeled SGS stresses, Eqs. 4.4 and 4.6, at the two filter levels to Eq. 4.10 to get:

$$\begin{aligned} \overline{T_{ij}}^{>2\epsilon} - \overline{\overline{\tau_{ij}}^{>\epsilon}}^{>2\epsilon} &\approx \overline{T_{ij}^M}^{>2\epsilon} - \overline{\overline{\tau_{ij}^M}^{>\epsilon}}^{>2\epsilon} \\ &= 2C_s(2\epsilon)^2 \left|\overline{S}^{>2\epsilon}\right| \overline{S_{ij}}^{>2\epsilon} - 2C_s\epsilon^2 \overline{\left|\overline{S}^{>\epsilon}\right| \overline{S_{ij}}^{>\epsilon}}^{>2\epsilon} . \end{aligned} \tag{4.11}$$

Following Lilly's (Lilly 1992) notation we define L_{ij} and M_{ij} as follows:

$$L_{ij} = \overline{\overline{u_i}^{>\epsilon} \overline{u_j}^{>\epsilon}}^{>2\epsilon} - \overline{\overline{u_i}^{>\epsilon}}^{>2\epsilon} \overline{\overline{u_j}^{>\epsilon}}^{>2\epsilon} , \tag{4.12}$$

$$M_{ij} = 2\epsilon^2 \overline{\left|\overline{S}^{>\epsilon}\right| \overline{S_{ij}}^{>\epsilon}}^{>2\epsilon} - 2(2\epsilon)^2 \left|\overline{S}^{>2\epsilon}\right| \overline{S_{ij}}^{>2\epsilon} , \tag{4.13}$$

where L_{ij} is a wavelet filtered analog to the Leonard stress. This results in an overdetermined system of equations that can be used to determine C_s

$$C_s M_{ij} = L_{ij} . \tag{4.14}$$

Following Lilly's (Lilly 1992) least square solution to this system, we obtain the following expression for the local Smagorinsky model coefficient:

$$C_s = \frac{L_{ij} M_{ij}}{M_{ij} M_{ij}} . \tag{4.15}$$

With this model formulation C_s can be locally positive or negative allowing for local backscatter. In practice it has been found that locally negative values of C_s cause numerical instabilities in SCALES, as in LES, so we average over the domain:

$$C_s = \frac{\langle L_{ij} M_{ij} \rangle}{\langle M_{ij} M_{ij} \rangle} , \tag{4.16}$$

where $\langle\cdot\rangle$ denotes volume averaging.

4.2. *Model Scaling*

If we make the assumption that, with an appropriate value for α, the eddy viscosity model (Eq.4.4-4.6) provides the right dissipation it is easy to show,

$$2C_s\epsilon^\alpha = -\frac{\tau_{ij}\overline{S}_{ij}^{>\epsilon}}{\left|\overline{S}^{>\epsilon}\right|\overline{S}_{ij}^{>\epsilon}\overline{S}_{ij}^{>\epsilon}}\,, \tag{4.17}$$

where α is the scaling law. Thus assuming α dependence we determine the correct scaling based on *a priori* testing, using a turbulent field obtained from a 256^3 DNS simulation of forced isotropic turbulence (Jimenez *et al.* 1993) with $\mathrm{Re}_\lambda = 168$. Note that this turbulent field will hereafter be referred to as F_{256}. In Figure 2 the scaling of $-\tau_{ij}\overline{S}_{ij}^{>\epsilon}/(\left|\overline{S}^{>\epsilon}\right|\overline{S}_{ij}^{>\epsilon}\overline{S}_{ij}^{>\epsilon})$ is shown over a range of $\epsilon/\left|\left|u\right|\right|_\infty$ that corresponds to a field compression over the range of 78.5% to 99.95%. The slope of the curve in log-log axis determines the appropriate ϵ scaling. As can be seen, the quantity $(-\tau_{ij}\overline{S}_{ij}^{>\epsilon}/(\left|\overline{S}^{>\epsilon}\right|\overline{S}_{ij}^{>\epsilon}\overline{S}_{ij}^{>\epsilon}))$ scales roughly as ϵ^2 for a wide range of compressions. However some deviation from this scaling is observed above 99.4% compression. Based on this *a priori* test of scaling, the new dynamic Smagorinsky-type eddy viscosity model (Eq. 4.4) has been implemented. The results of simulations with this new SGS model are shown in Section 5.

5. Results

To validate the SCALES method, numerical simulations of decaying incompressible isotropic turbulence are considered. For this work the incompressible Navier Stokes equations (Eqs. 4.1-4.3) are solved with the DAWC solver. Continuity (Eq. 4.3) is enforced using a multi-step pressure correction time integration method (Guermond & Shen 2003). An adaptive wavelet collocation multilevel elliptic solver (Vasilyev & Kevlahan 2003) is used in solving the Poisson equation for pressure at each time step.

Results of decaying incompressible isotropic turbulence with initial $\mathrm{Re}_\lambda = 72$ are presented. The simulations were initialized with a 128^3 forced isotropic turbulence DNS field from a de-aliased pseudo-spectral code. The spectral content of the initial DNS field is fully resolved by doubling the non-adaptive field resolution to 256^3 in the simulations. This is required because the DAWC solver uses finite differencing, which is not adequate for resolving the full spectral content of the spectral DNS field at the original resolution. The results are compared to DNS of decaying isotropic turbulence performed with the same de-aliased pseudo-spectral code used to generate the initial DNS field.

In running these simulations it has been determined that a more conservative adjacent zone, then the one described in Section 3, was needed to limit the numerical and aliasing error at the high field compression used in SCALES. In the original adjacent zone neighboring points on the level above, the current level, and the level below are added around each active wavelet. We will call this a non-conservative adjacent zone. For the high compression SCALES simulations we have defined a conservative adjacent zone that, in addition to the immediate neighbors, adds the diagonal neighbors. For high Reynolds numbers the coherent structures in the flow become more localized and the overhead associated with this conservative adjacent zone will be considerably reduced.

In these simulations a normalized wavelet threshold is specified. The wavelet threshold

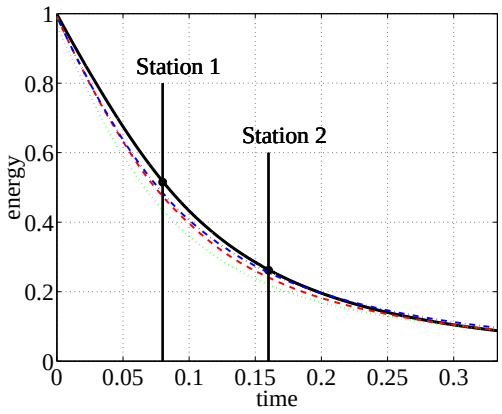

FIGURE 3. Energy decay for $\text{Case}_{\text{Re}_\lambda=72}$ with conservative adjacent zone for SCALES with dynamic SGS model (– – – –), SCALES with SGS model coefficient $C_s\epsilon^2 = 0.0001$ (— — —), LES with dynamic SGS model (·····) and for comparison DNS (———). Two stations are shown at which energy spectra will be presented.

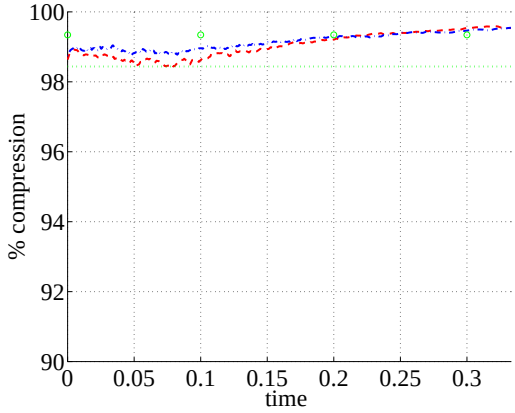

FIGURE 4. Field compression for $\text{Case}_{\text{Re}_\lambda=72}$ with conservative adjacent zone for SCALES with dynamic SGS model (– – – –), SCALES with SGS model coefficient $C_s\epsilon^2 = 0.0001$ (— — —) and LES with dynamic SGS model (·····). The more conservative interpretation of the LES compression based on the 3/2 rule is shown as small circles.

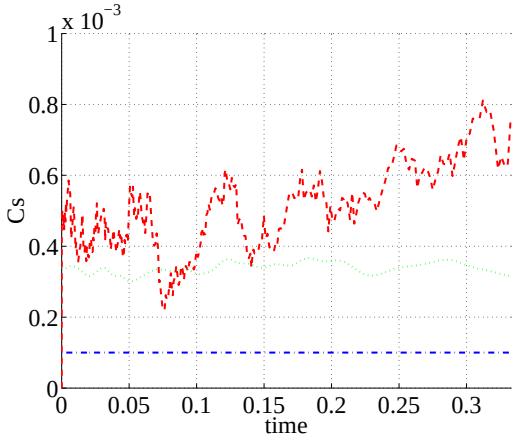

FIGURE 5. Dynamic SGS model coefficient for $\text{Case}_{\text{Re}_\lambda=72}$ with conservative adjacent zone for SCALES with dynamic SGS model (– – – –), SCALES with SGS model coefficient $C_s\epsilon^2 = 0.0001$ (— — —) and LES with dynamic SGS model (·····).

is specified as relative to the L_2 norm of the velocity field. During the simulation the relative wavelet threshold ϵ_2 is specified for the whole simulation and the actual absolute wavelet threshold used at each time step is $\epsilon = \epsilon_2 \, ||u||_2$.

5.0.1. *SCALES Constant Coefficient and Dynamic SGS Stress Model*

SCALES simulations have been performed with the constant coefficient Smagorinsky eddy viscosity model (Eq. 4.4) and the new dynamic Smagorinsky eddy viscosity SGS stress model described in Section 4.1. The model coefficient ($C_s\epsilon^2 = 0.0001$) for the

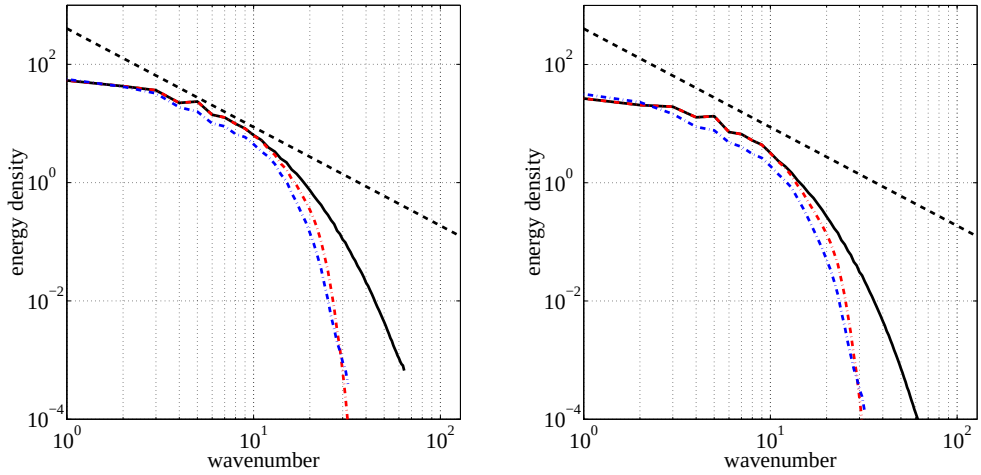

FIGURE 6. Energy spectra for $\text{Case}_{\text{Re}_\lambda=72}$ with conservative adjacent zone for LES with dynamic SGS model (– – –) at time $t = 0.08$ (left), and $t = 0.16$ (right). For comparison the DNS (———) and filtered DNS (– – – –) are shown. A $k^{-5/3}$ straight dashed black line is shown to indicate the inertial range.

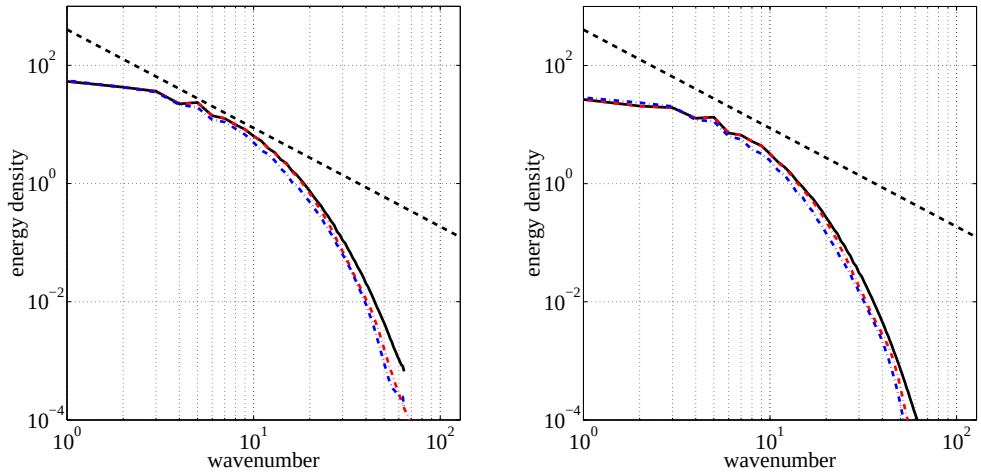

FIGURE 7. Energy spectra for $\text{Case}_{\text{Re}_\lambda=72}$ with conservative adjacent zone for SCALES with SGS model coefficient $C_s\epsilon^2 = 0.0001$ (– – –) at time $t = 0.08$ (left), and $t = 0.16$ (right). For comparison the DNS (———) and filtered DNS (– – – –) are shown. A $k^{-5/3}$ straight dashed black line is shown to indicate the inertial range.

$\text{SCALES}_{\text{Cs}}$ case was chosen to best match the DNS results. For the $\text{SCALES}_{\text{dyn}}$ case the volume averaged version of the dynamic model coefficient is used (Eq. 4.16). These SCALES simulations, hereafter for brevity called $\text{SCALES}_{\text{Cs}}$ and $\text{SCALES}_{\text{dyn}}$ respectively, are compared to DNS and LES simulations. For both $\text{SCALES}_{\text{Cs}}$ and $\text{SCALES}_{\text{dyn}}$ cases ϵ_2 is set to 0.5. The LES simulation is performed in the DAWC solver with a regular 64^3 grid. The simulation is de-aliased by performing a wavelet transform on the

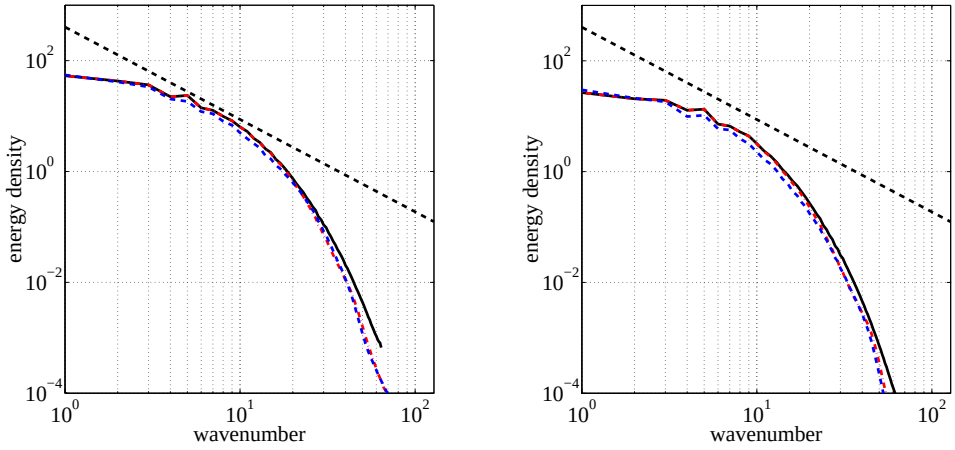

FIGURE 8. Energy spectra for $\text{Case}_{\text{Re}_\lambda=72}$ with conservative adjacent zone for SCALES with dynamic SGS model (— - —) at time $t = 0.08$ (left), and $t = 0.16$ (right). For comparison the DNS (———) and filtered DNS (- - - -) are shown. A $k^{-5/3}$ straight dashed black line is shown to indicate the inertial range.

velocity field and zeroing the highest level wavelet coefficients, thus resulting in a 32^3 solution at the end of the time step. This is more expensive than would be required in a spectral code using the 3/2 rule. In Figure 3 it can be seen that the resolved kinetic energy decay for the $\text{SCALES}_{\text{dyn}}$ and $\text{SCALES}_{\text{Cs}}$ cases closely matches that of the DNS. The LES deviates a small amount more from the DNS. In Figure 4 the compression for the $\text{SCALES}_{\text{dyn}}$, $\text{SCALES}_{\text{Cs}}$ and LES cases are shown. If we consider the overhead of the modes used for de-aliasing, the LES could be considered to have a compression of 98.44%. The modes used for de-aliasing in LES can be considered as analogous to the adjacent zone in SCALES so for a realistic comparison we can consider that if the LES was performed in a spectral code, using the 3/2 rule for de-aliasing, the effective compression would be 99.34% (shown in Fig. 4 as small circles). This is close to the initial compression of the $\text{SCALES}_{\text{dyn}}$ simulation, but as the SCALES simulations progress the compression increases. Therefore, it can be said that the $\text{SCALES}_{\text{dyn}}$ and $\text{SCALES}_{\text{Cs}}$ simulations were able to capture the energy decay with a compression similar to a de-aliased LES simulation. In Figure 5 we see that the dynamic model coefficient for $\text{SCALES}_{\text{dyn}}$ is more variable in comparison to the LES case. It is hypothesized that this variability could be reflective of the sensitivity of the $\text{SCALES}_{\text{dyn}}$ model to actual localized events such as energetic coherent vortex interactions that cause local high resolved stresses that are reflective of the proper instantaneous SGS dissipation. Further research is needed to understand this phenomenon. In Figures 6-8 the energy spectra for the two stations shown in Figure 3 are compared to the appropriately filtered DNS for the $\text{SCALES}_{\text{dyn}}$, $\text{SCALES}_{\text{Cs}}$ and LES cases. It can be seen that, while there is reasonable agreement for the LES case (Fig. 6), the agreement with the filtered DNS is significantly improved for the $\text{SCALES}_{\text{Cs}}$ (Fig. 7) and $\text{SCALES}_{\text{dyn}}$ cases (Fig. 8). At both stations, in the dissipative range, the $\text{SCALES}_{\text{Cs}}$ and $\text{SCALES}_{\text{dyn}}$ simulations reproduce more of the high wave number energy. At the second station it can be seen in the inertial range that the LES has dissipated slightly more then the $\text{SCALES}_{\text{Cs}}$ and $\text{SCALES}_{\text{dyn}}$ cases. It is of

particular interest to note that the wavelet filtered DNS in Figures 7 and 8 are closer to the full DNS spectra over the full spectral range. Thus, the ability of SCALES to closely recover the filtered DNS, results in a solution that has a spectral content close to the original unfiltered DNS solution, over the whole DNS spectral range.

6. Conclusions

In this work dynamic simulation results of decaying incompressible isotropic turbulence using a new methodology for simulating turbulent flows called Stochastic Coherent Adaptive Large Eddy Simulation (SCALES) (Goldstein & Vasilyev 2004) are presented. The SCALES method has been implemented using a Dynamically Adaptive Wavelet Collocation (DAWC) method that is ideal for CVS, and SCALES as it combines the resolution of the energetic coherent modes in a turbulent flow with the simulation of their temporal evolution (Vasilyev 2003, Vasilyev & Bowman 2000, Kevlahan *et al.* 2003, Goldstein *et al.* 2003, Vasilyev & Kevlahan 2002).

In this work a new dynamic SGS stress modeling procedure has been introduced based on a variation of the classical Smagorinsky (Smagorinsky 1963) model formulation. In this model the scaling of the eddy viscosity is based on ϵ^2, instead of the standard scaling, $\overline{\Delta}^2$. *A priori* results using forced incompressible isotropic turbulence have been presented that show this scaling holds, for a wide range of compression. The new dynamic procedure is similar in spirit to the classical dynamic procedure of Germano's (Germano *et al.* 1991, Germano 1992), except that the new scaling law, based on ϵ^2, is used.

Dynamic simulations of SCALES and LES of decaying isotropic turbulence with a Taylor Reynolds number of $\mathrm{Re}_\lambda = 72$ have been have been compared to DNS results to validate the SCALES method with the DAWC solver. Dynamic SCALES simulations, using the new dynamic modeling procedure, are performed with an expanded adjacent zone to reduce aliasing and numerical error at high wavelet compression. The SCALES results with the dynamic model are shown to reproduce the DNS energy decay with only 1 % of the modes being initially resolved. It is anticipated that in higher Reynolds number simulations the cost of this conservative adjacent zone will become minimal. These SCALES results are also compared to fully de-aliased LES calculations. The SCALES results moderately outperformed those of the LES at a similar field compression.

While it is expected that for Reynolds numbers higher than the ones considered in this study the reduced SGS dissipation and increased incoherency of the SCALES SGS stress will provide a tangible improvement in SGS model accuracy, this is not in and of itself the greatest potential benefit of the SCALES method. Real world flows of engineering and scientific interest occur in complex domains with great temporal and spatial variation in turbulence intensity. Therefore, an efficient simulation method must be capable of dynamically, often with limited *a priori* knowledge, adapting to the local resolution over a wide range of Reynolds numbers often including large regions of laminar flow. A good example of this is flow over a modern aircraft that spans the gamut of flows from a nearly laminar far field to areas of intense turbulence in the control surfaces regions. Another area of great potential benefit is in the simulation of fluid structure interaction, where, often no detailed *a priori* information to build cost effective computational grids is available. Therefore, the trade off between costly grid refinement over regions of potentially high turbulence intensity versus the loss of simulation accuracy must be weighed. With the SCALES methodology the collocation grid automatically adapts to the local flow in order to maintain an *a priori* described accuracy threshold, which is the *a priori*

determined wavelet filter threshold (ϵ). For these reasons even if the SCALES methodology can do no better than match the cost of classical LES methods in unit test problems, like the ones conducted in this work, there is strong evidence to believe that SCALES will be able to outperform classical LES in many complex real world flows. To realize the benefits of SCALES in such highly non-homogenous flows in complex geometries a local SGS model will be required. Work on such a model is currently underway.

7. Bibliography

REFERENCES

Daubechies, I., 1992, *Ten Lectures on Wavelets*, no. 61 in CBMS-NSF Series in Applied Mathematics, SIAM, Philadelphia.

Donoho, D., 1993, Unconditional bases are optimal bases for data compression and for statistical estimation., *Appl. Comput. Harmon. Anal.*, **1**, 100–115.

Donoho, D. L., 1992, Interpolating wavelet transforms, Tech. Rep. 408, Department of Statistics, Stanford University.

Donoho, D. L., 1994, De-noising by soft-thresholding, *IEEE Trans. Inf. Theory*, **41**(3), 613–627.

Farge, M., Schneider, K., & Kevlahan, N., 1999, Non-Gaussianity and coherent vortex simulation for two-dimensional turbulence using an adaptive orthogonal wavelet basis, *Phys. Fluids.*, **11**(8), 2187–2201.

Farge, M., Pellegrino, G., & Schneider, K., 2001, Coherent vortex extraction in 3d turbulent flows using orthogonal wavelets, *Physical Review Letters*, **87**(5).

Germano, M., 1992, Turbulence: the filtering approach, *J, Fluid Mech.*, **238**, 325–336.

Germano, M., Piomelli, U., Moin, P., & Cabot, W., 1991, A dynamic subgrid-scale eddy viscosity model, *Phys. Fluids A*, **3**(7), 1760–1765.

Goldstein, D. A. & Vasilyev, O. V., 2004, Stochastic coherent adaptive large eddy simulation method, *Phys. Fluids*, **16**(7), 2497–2513.

Goldstein, D. A., Vasilyev, O. V., & Kevlahan, N.-R., 2003, Feasibility study of an adaptive large eddy simulation method, *AIAA Paper 2003-3551*.

Guermond, J.-L. & Shen, J., 2003, Velocity-correction projection methods for incompressible flows, *To appear in SIAM J. Num. Anal.*, **41**(1), 112–134.

Jimenez, J., Wray, A., Saffman, P., & Rogallo, R., 1993, The structure of intense vorticity in isotropic turbulence, *J. Fluid Mech.*, **225**, 65–90.

Kevlahan, N. & Ghidaglia, J.-M., 2001, Computation of turbulent flow past an array of cylinders using a spectral method with Brinkman penalization, *Eur. J. Mech./B*, **B 20**, 333–350.

Kevlahan, N. K.-R., Vasilyev, O. V., & Goldstein, D. E., 2003, A three-dimensional adaptive wavelet method for fluid-structure interaction, in *Proceedings of Direct and Large-Eddy Simulation Workshop 5*, Technical University of Munich, Germany.

Lilly, D. K., 1992, A proposed modification to the germano subgrid-scale closure model, *Phys. Fluid*, **3**, 633–635.

Mallat, S. G., 1999, *A Wavelet Tour of Signal Processing*, Academic Press, Paris.

Smagorinsky, J. S., 1963, General circulation experiments with the primitive equations, *Mon. Weather Rev.*, **91**, 99–164.

Sweldens, W., 1996, The lifting scheme: A custom-design construction of biorthogonal wavelets, *Appl. Comput. Harmon. Anal.*, **3**(2), 186–200.

Sweldens, W., 1998, The lifting scheme: A construction of second generation wavelets, *SIAM J. Math. Anal.*, **29**(2), 511–546.

Vasilyev, O. V., 2002, Solving multi-dimensional evolution problems with localized structures using second generation wavelets, *Int. J. Comp. Fluid Dyn.,* Special issue on High-resolution methods in Computational Fluid Dynamics, **17**(2), 151–168.

Vasilyev, O. V., 2003, Solving multi-dimensional evolution problems with localized structures using second generation wavelets, *Int. J. Comp. Fluid Dyn.,* Special issue on High-resolution methods in Computational Fluid Dynamics, **17**(2), 151–168.

Vasilyev, O. V. & Bowman, C., 2000, Second generation wavelet collocation method for the solution of partial differential equations, *J. Comp. Phys.*, **165**, 660–693.

Vasilyev, O. V. & Kevlahan, N. K.-R., 2002, Hybrid wavelet collocation - Brinkman penalization method for complex geometry flows, *Int. J. Numerical Methods in Fluids*, **40**, 531–538.

Vasilyev, O. V. & Kevlahan, N. K.-R., 2003, An adaptive multilevel wavelet collocation method for elliptic problems, Submitted to *J. Comp. Phys.*

Vasilyev, O. V. & Paolucci, S., 1996, A dynamically adaptive multilevel wavelet collocation method for solving partial differential equations in a finite domain, *J. Comput. Phys.*, **125**, 498–512.

Vasilyev, O. V. & Paolucci, S., 1997, A fast adaptive wavelet collocation algorithm for multi-dimensional PDEs, *J. Comput. Phys.*, **125**, 16–56.

Vasilyev, O. V., Yuen, D. A., & Paolucci, S., 1997, The solution of PDEs using wavelets, *Computers in Phys.*, **11**(5), 429–435.

Vasilyev, O. V., Podladchikov, Y. Y., & Yuen, D. A., 1998, Modeling of compaction driven flow in poro-viscoelastic medium using adaptive wavelet collocation method, *Geophys. Res. Lett.*, **25**(17), 3239–3242.

Vasilyev, O. V., Podladchikov, Y. Y., & Yuen, D. A., 2001, Modeling of viscoelastic plume-lithosphere interaction using adaptive multilevel wavelet collocation method, *Geophys. J. Int.*, **147**(3), 579–589.